

Potential for mono-cast material to achieve high efficiencies in mass production

Milica Mrcarica, Photovoltech NV, Tienen, Belgium

ABSTRACT

Despite the drop in price of silicon wafers, they are still one of the main factors influencing the cost and performance of Si-based solar cells. These two consequences have initiated a growing commercial interest in mono-cast (cast-mono, mono-like or quasi-mono) Si wafers, supported by R&D in the areas of material characterization, correlation with cell efficiencies, and mono-cast material use in advanced cell technologies. This paper gives a broad overview and comparison of commercially available grades of mono-cast material from different suppliers. The performance of the material from production in high-throughput screen-printing lines, as well as an analysis of the main material characteristics influencing these results, is presented. A characterization using a lifetime tester and a photoluminescence (PL) imaging tool has shown that not only grain boundaries but also dislocations could cause a drop in cell V_{oc} of more than 15mV. Wafers with large surface areas of $\langle 100 \rangle$ Si lattice planes, when processed with anisotropic texturing, could yield an increase in I_{sc} greater than 400mA for 6" substrates, as compared to the isotropic-textured equivalents. Furthermore, when a high-grade mono-cast material processed in anisotropic texturing was compared with CZ mono material from the same supplier and of the same resistivity, light-induced degradation (LID), presented as combined V_{oc} and I_{sc} degradation, was only one-third of that in CZ material. However, although mono-cast material has the potential to increase cell line performance to the same level as that gained by important process and technological improvements, it imposes very high requirements for better material sorting in order to achieve stable cell electrical performance and module aesthetics acceptable to the market.

Introduction

According to the SEMI ITRPV [1], Si wafers represent more than 50% of the final cell cost. It is envisaged that a reduction of this cost will happen not only by reducing wafer thickness, but also by improving material quality – mainly multicrystalline Si (mc-Si) – so that J_{0bulk} is reduced from 600 to 200fA/cm² by the year 2020. The producers of mc-Si wafers are taking two paths to reach this target. One is the improvement of the casting conditions for high-performance mc-Si (HPM) wafers [2]. A more promising path, however, is the casting of Si material with large grains of $\langle 100 \rangle$ orientation (mono-casting), first announced by BP Solar in 2006 [3]; more recently, dendritic growth research was reported by IMT and Kyoto University Japan in 2009 [4,5].

Mono-casting technology has been commercialized through the development of silicon monocrystalline growth casting furnaces [6]. High-throughput production using the mono-casting approach is now under way at GCL, LDK, ReneSola, Pillar, JA Solar and other silicon ingot and cell manufacturing companies [7,8]. Although the suppliers of mono-cast material claim an increase in cell efficiency of up to 1% absolute, and a reduction in light-induced degradation (LID) and cell-to-module (CTM) losses, mono-cast does not have a significant share in mass cell production. The ITRPV sees the share of mono-cast increasing to 50% by the year 2020.

The growing commercial interest in mono-cast material has been supported by R&D in the area of its impact on cell

performance and material characterization [9–11], as well as its use in advanced technologies [12,13]. A promising result of 20.2% efficiency for n-type premium-grade mono-cast material with a heterojunction cell concept has been published [14].

“The ITRPV sees the share of mono-cast increasing to 50% by the year 2020.”

Comparison of supplier materials in production

Table 1 presents the different suppliers' classes of mono-cast wafers covered in this

Wafer supplier	Tested classes	Mono $\langle 100 \rangle$ Area (M)			Ingot split			Wafering process	Texturing	
		Class 1	Class 2	Class 3	Class 1	Class 2	Class 3		Isotropic	Anisotropic
A	C1,C2,C3	$M \geq 90\%$	$70\% \leq M < 90\%$	$M \leq 70\%$	25%	15%	60%	Wire saw	C1	C1,C2,C3
B*	C1,C2,C3	$M \geq 90\%$	$70\% \leq M < 90\%$	$M \leq 70\%$	57%	29%	14%	Wire saw		C1,C2,C3
C	C1,C2,C4	$M \geq 90\%$	$40\% \leq M < 90\%$	$M \leq 40\%$	30%	40%	30%	Wire saw		C1,C2,C3
D	C2,C3	$M \geq 85\%$	$70\% \leq M < 85\%$	$20\% \leq M < 70\%$	Unknown			Wire saw		C2,C3
E**	C1	$M = 100\%$	N/A	N/A	100%			Diamond wire saw	C1	

* Supplier B, a standard supplier of mc-Si wafers, was used as a benchmark in this study

** Material not commercially available

Table 1. A review of the suppliers' classes, the ingot split as indicated by the suppliers, and the wafering and texturing processes.

work. Before shipment of the material, the classes are sorted visually by the suppliers on the basis of the ratio or percentage of <100> area on the wafer. This sorting of the material into classes by the suppliers is qualitative and results in high variations within the batch, from batch to batch, and from supplier to supplier.

Electrical performance

Evaluating the different mono-cast wafer classes and suppliers and benchmarking against mc-Si material in production was a challenging task. It is well known from production practice that mc-Si wafer variations and/or process noise could result in significant differences in cell line

performance on different occasions, even for the same wafer supplier. Production runs were performed on the same production screen-printing line, and with a process set-up for mc-Si material using batch isotropic texturing. At that stage, no attempt was made to optimize the process for different materials; an exception was

Wafer supplier	Variable Class	Abs Δ efficiency [%]				Abs Δ V_{oc} [mV]				Abs Δ I_{sc} [A]				Abs Δ FF [%]			
		Mean	Min	Max	STD	Mean	Min	Max	STD	Mean	Min	Max	STD	Mean	Min	Max	STD
A	1	0.58	-1.73	1.21	0.37	7.46	-21.93	15.88	4.72	0.15	-0.63	0.33	0.10	0.41	-5.02	1.31	0.41
	2	0.26	-2.58	1.12	0.42	2.56	-26.08	14.98	5.95	0.08	-0.97	0.31	0.11	0.16	-3.40	1.27	0.47
	3	0.02	-4.65	1.11	0.34	-1.00	-28.64	14.46	5.05	0.03	-2.20	0.28	0.09	-0.10	-11.99	1.09	0.46
B	1	0.52	-0.41	0.93	0.23	8.49	-4.14	13.02	2.30	0.14	-0.13	0.25	0.06	0.12	-1.31	0.87	0.29
	2	0.28	-0.18	0.81	0.36	5.18	-1.08	12.59	5.09	0.07	-0.08	0.22	0.10	-0.01	-0.93	0.51	0.27
	3	-0.13	-0.77	0.56	0.30	-1.00	-6.75	8.32	4.03	-0.05	-0.20	0.14	0.09	0.00	-1.91	0.35	0.24
C	1	0.48	-0.72	1.02	0.49	7.58	-5.14	13.86	6.45	0.23	-0.04	0.37	0.14	-0.84	-3.04	-0.25	0.45
	2	0.28	-1.18	0.85	0.34	4.37	-4.85	11.29	4.14	0.18	-0.04	0.34	0.10	-0.87	-4.82	-0.31	0.53
	3	0.03	-0.60	0.69	0.23	-0.07	-4.55	8.39	2.69	0.09	-0.03	0.26	0.06	-0.72	-4.57	-0.09	0.48
D	2	0.24	-0.42	0.76	0.26	4.88	-3.97	11.46	3.48	0.05	-0.12	0.21	0.07	0.03	-1.44	0.60	0.25
	3	0.11	-0.70	0.43	0.19	0.27	-12.50	4.75	2.96	0.14	0.04	0.24	0.05	-0.77	-2.48	-0.12	0.50
E*	1	0.80	-0.42	1.27	0.28	-1.14	-8.67	5.86	3.27	0.38	-0.11	0.51	0.09	0.36	-1.17	0.96	0.37
B	mc-Si	0.00	-1.98	0.70	0.33	0.00	-23.72	12.91	5.40	0.00	-0.39	0.17	0.08	0.00	-7.95	0.78	0.51

* Group E, diamond wire saw, anisotropic texturing

Table 2. Absolute changes in efficiency, V_{oc} , I_{sc} and fill factor (FF) for the different classes of mono-cast wafers from various suppliers. The values are normalized to the mc-Si material from supplier B, used as the standard wafer supplier on the production line.

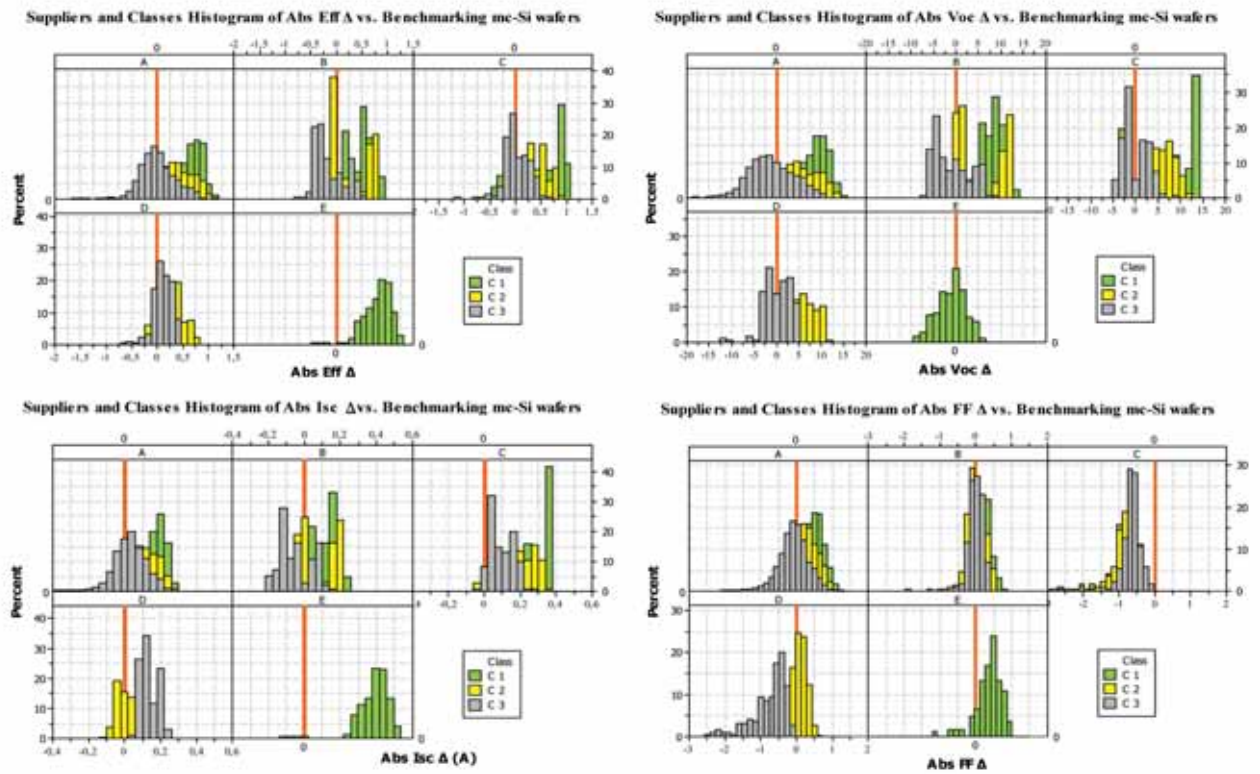


Figure 1. Distribution of the absolute efficiency, V_{oc} , I_{sc} and FF differences compared with the average values for the performance of mc-Si wafers from supplier B (denoted by reference line 0 in red).

the material from supplier E, to which in-line anisotropic texturing was applied. The mc-Si material from supplier B (used for comparison purposes in this analysis and a standard material in production) was evaluated and averaged over different production times and batches.

The advantages of mono-cast material became apparent: a significant increase (especially for the premium class) in V_{oc} of up to 9mV and in I_{sc} of to 230mA for isotropic textured wafers. The enhanced I_{sc} of 380mA for supplier E results from the low reflectance achieved by the anisotropic texturing process. The change in FF was not systematic and depends more on the process variation or non-optimized process for different wafer materials. The electrical property results are summarized in Table 2.

The improvement in overall performance of mono-cast material is also due to the distribution shift towards higher performing cell bins, as shown in Fig. 1. Supplier A has the highest spread in V_{oc} and I_{sc} , but also

the best potential for achieving the highest values in V_{oc} and I_{sc} . Suppliers A, B and C show drops in V_{oc} and I_{sc} for class 3, and supplier E even for class 1, compared with mc-Si wafers. This is not the case, however, for supplier D, which also exhibits the lowest variation in V_{oc} and I_{sc} . For all the classes from all the suppliers, mono-cast material demonstrates a high variation and spread inside each class, sometimes even higher than mc-Si material. This outcome is due not only to the lack of suitable sorting but also to the high variation in internal material structure.

Understanding material structure and its influence on cell performance

A Sinton instruments WCT-IL800 in-line tool was used for lifetime, resistivity and trap density measurements of the representative groups of as-cut wafers. Table 3 presents a summary of the wafer resistivity

and lifetime measurements; the distribution of wafer trap density is shown in Fig. 2.

There was no direct correlation between the as-cut wafers' resistivity, lifetime and trap density and the cells' electrical performance: suppliers A and C have higher resistivities and lifetimes, but not higher gains in V_{oc} and I_{sc} . Variations in resistivity and lifetime, however, seem to be contributors to the variations in V_{oc} and I_{sc} : supplier E and D show lower STDs for wafer and cell performance. Further and more detailed study of well-sorted wafers could provide a better understanding of these dependencies.

“There was no direct correlation between the as-cut wafers' resistivity, lifetime and trap density and the cells' electrical performance.”

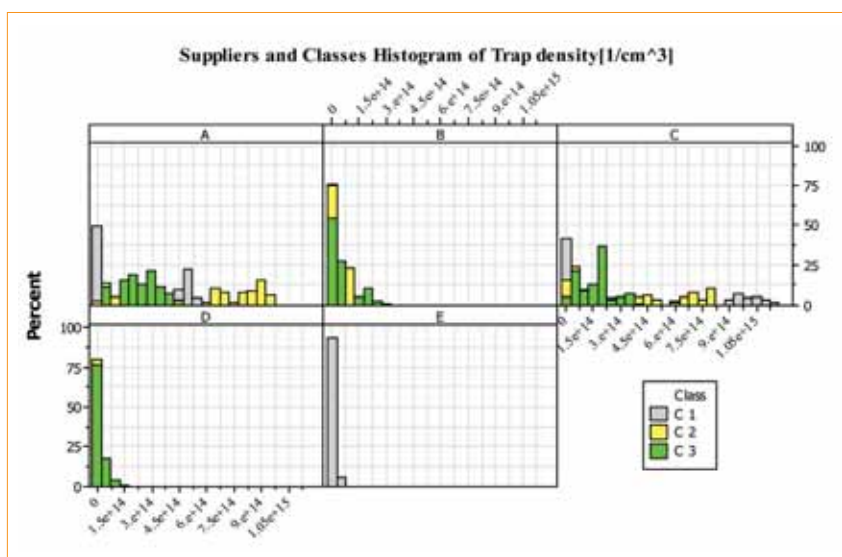


Figure 2. Trap density measurements from in-line testing for the different suppliers and classes of as-cut wafers.

The photoluminescence (PL) analysis was performed on a BT Imaging tool LIS-R1. For supplier C, PL imaging and J_0 imaging was done using a PLpix system from Solar Centrum Institute of Stuttgart. The PL imaging carried out on selected wafers and cells of suppliers and classes reveals the internal material structure and its impact on the finished cell, as shown in Fig. 3.

The same classes from different suppliers show similar structures. For supplier A, the wafer grain boundaries decrease in the premium classes, and the level of dislocations is low. Wafers with an entire area of $\langle 100 \rangle$ show the positions of the CZ seed plates from casting, but these dislocations do not have a significant impact on cell performance. The structure for supplier B is similar to that for supplier A (as shown in the PL images for as-cut wafers): depending on

Wafer supplier	Variable		Resistivity [Ωcm]				Lifetime [μs]			
	Class	Mean	Min	Max	STD	Mean	Min	Max	STD	
A	1	2.01	1.70	2.60	0.33	0.98	0.84	1.11	0.06	
	2	2.17	1.60	2.60	0.31	1.00	0.79	1.11	0.05	
	3	1.99	1.80	2.40	0.13	0.95	0.71	1.03	0.05	
B	1	1.34	1.21	1.47	0.07	0.86	0.44	0.94	0.06	
	2	1.33	1.13	1.63	0.11	0.79	0.26	1.01	0.16	
	3	1.26	1.08	1.42	0.08	0.80	0.65	0.90	0.05	
C	1	2.11	1.71	2.55	0.22	0.93	0.62	1.17	0.11	
	2	2.22	1.86	2.91	0.26	1.03	0.89	1.14	0.06	
	3	1.94	1.58	2.50	0.17	0.92	0.61	1.07	0.09	
D	2	1.54	1.30	1.80	0.12	0.91	0.74	1.03	0.05	
	3	1.50	1.00	1.80	0.14	0.88	0.65	1.03	0.08	
E	1	1.54	1.40	1.70	0.08	0.88	0.80	0.94	0.03	

Table 3. Summary of resistivity and lifetime measurements from in-line testing for different suppliers and classes of as-cut wafers.

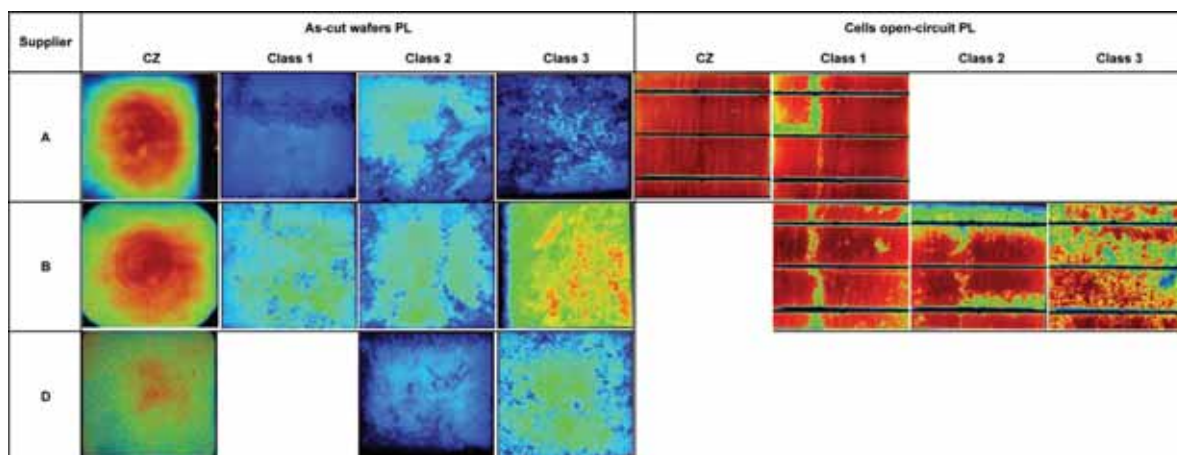
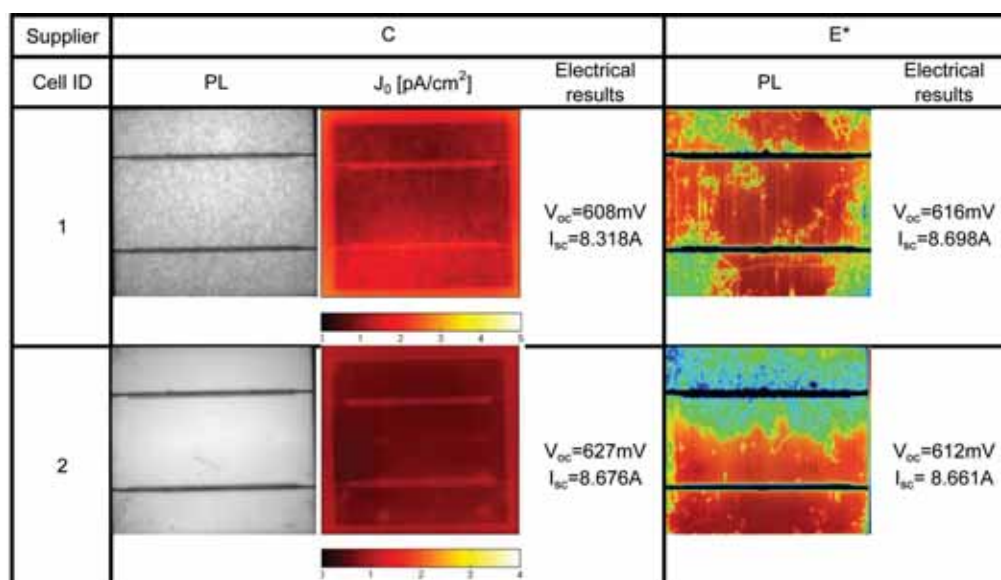


Figure 3. Uncalibrated PL images of the as-cut wafers of different classes from various suppliers (left) and PL images of representative cells (right). CZ and class 1 cells had anisotropic texturing. For supplier A, CZ cell efficiency = 18.54% and class 1 cell efficiency = 18.42%.



*Anisotropic texturing

Figure 4. PL images and corresponding V_{oc} and I_{sc} for finished cells from suppliers C and E created from the wafers with single crystal appearance.

the class, the grain boundaries decrease and the level of dislocations is variable. Supplier D is similar to supplier A but has fewer grain boundaries in class 3 than in the same class of supplier A. Supplier C has a large number of wafers in class 1 with the appearance of single $\langle 100 \rangle$ crystal. These wafers have the potential to yield high I_{sc} and V_{oc} , even with isotropic texturing.

Some of the wafers from certain batches, however, show a high level of dislocation, which is detrimental to V_{oc} and J_0 , as shown in Fig. 4. Supplier E's wafers also have the single crystal appearance and no grain boundaries, but a high level of dislocation, decreasing V_{oc} to the same level as (or below) that for mc-Si wafers (Fig. 4). The efficiency of supplier E is above 17% because of anisotropic texturing, resulting in low cell reflectance.

Achieving high efficiencies with mono-cast wafers

Smaller-scale groups of supplier B classes 1–3 and supplier A class 1 were processed through isotropic texturing and under similar process conditions to those for cell line set-up using standard screen-printing technology. These groups were compared with supplier A class 1 mono-cast and supplier A CZ wafers processed through an in-line anisotropic texturing process. All wafers had between 1.5 Ωcm and 2.0 Ωcm resistivity. The results are shown in Fig. 5.

Supplier A's wafers have a narrower distribution and better performance than high-grade wafers from supplier B; however, the top group of wafers in B produced efficiencies close to 18% without anisotropic texturing and yielded a V_{oc} of

632mV. A comparison of different grades of material has confirmed once again the critical impact of material structure on cell performance, as well as the need for a good wafer-sorting system.

Performing anisotropic texturing on class 1 mono-cast wafers has an impact on I_{sc} , and thus on efficiency, which is greater than that gained by a change in class of mono-cast wafer. The increase in efficiency is greater than 0.8% absolute with anisotropic texturing compared to isotropic texturing. This improvement, driven by an increase in I_{sc} of 420mA at the cell level with reference to isotropic texturing, is remarkable and of greater impact than the difference between mono-cast material of class 1 and CZ material. Mono CZ wafers have a higher V_{oc} (by 2mV) than mono-cast, and similar I_{sc} .

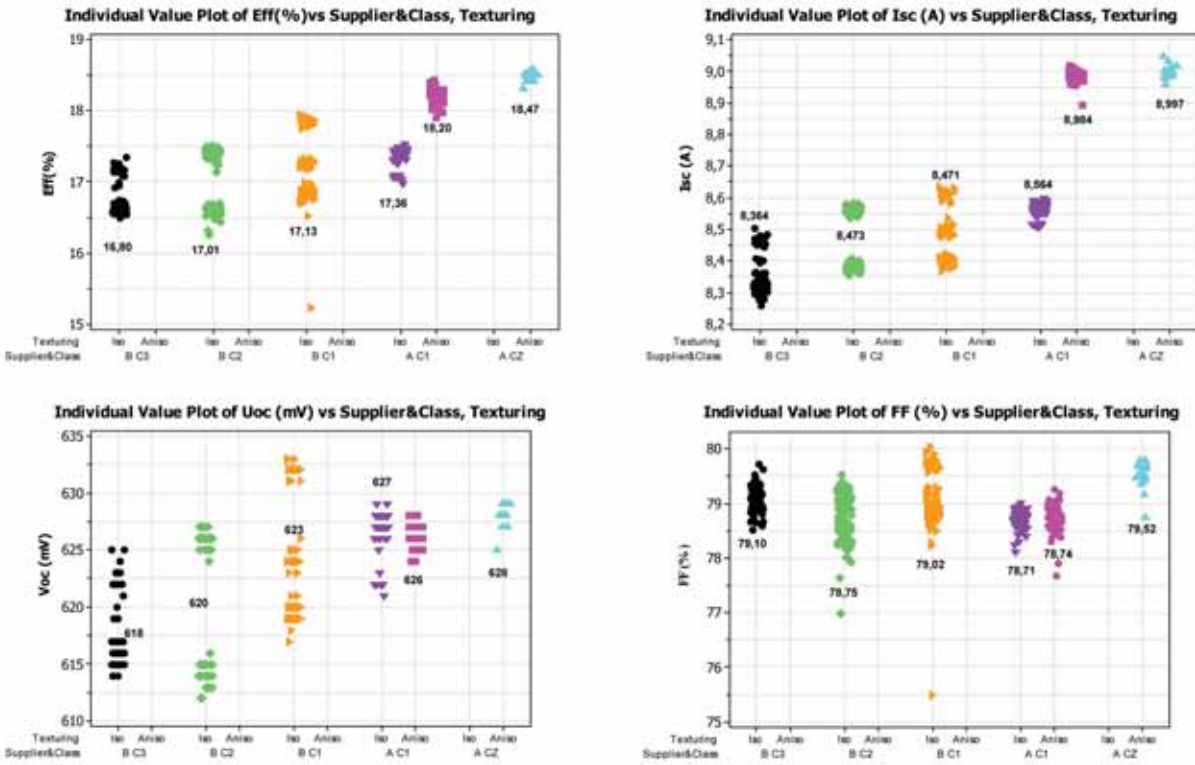


Figure 5. Comparison of the electrical performance of isotropic texturing groups of classes 1–3 of mono-cast wafers from supplier B and class 1 from supplier A, with anisotropic texturing groups of class 1 mono-cast and CZ material from supplier A.

“The anisotropic texturing process offers the highest potential for improving mono-cast efficiency.”

The anisotropic texturing process offers the highest potential for improving mono-cast efficiency because it is possible to have almost the whole surface with <111> orientation and low reflectance. However, for the grains with different orientations, this could cause cosmetic issues at the cell and module levels, owing to the significant reflectance range at the wafer level and at the wafer to wafer level. It is for this reason that texturing of mono-cast material (and

Cell ID	Supplier	Class	Texture	$I_{sc} \Delta$ [%]	$V_{oc} \Delta$ [%]	Total Δ [%]
A CZ #1a	A	CZ	Anisotropic	-0.94	-0.78	-1.71
A CZ #2a	A	CZ	Anisotropic	-0.88	-0.59	-1.47
A C1#1a	A	C1	Anisotropic	-0.34	-0.08	-0.42
A C1#2a	A	C1	Anisotropic	-0.47	-0.16	-0.62
A C1#1	A	C1	Isotropic	-0.29	-0.10	-0.38
A C1#2	A	C1	Isotropic	-0.36	-0.22	-0.58
B C1#1	B	C1	Isotropic	-0.47	-0.08	-0.55
B C1#2	B	C1	Isotropic	-0.65	-0.19	-0.84
B C3#1	B	C3	Isotropic	-0.30	-0.06	-0.37
B C3#2	B	C3	Isotropic	-0.44	-0.11	-0.55
CZ average				-0.91	-0.68	-1.59
Mono-cast average				-0.42	-0.13	-0.54

Table 4. Response to LID of mono-cast wafers and CZ wafers with 1.5–2.0Ωcm resistivities.

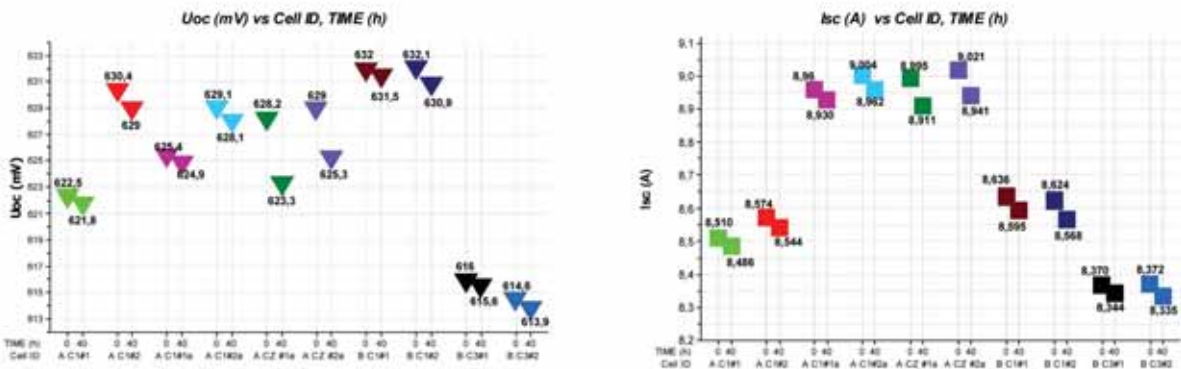


Figure 6. I_{sc} and V_{oc} before and after 40 hours' light-soaking for mono-cast material from suppliers A and B, and CZ material from supplier A.

the texturing impact on different mono-cast classes) and reflectance have recently been studied in more detail and new texturing chemistries to reduce the above-mentioned differences proposed [15–17].

Quantifying the LID effect for mono-cast materials

In order to confirm that the mono-cast classes and suppliers have no impact on the LID effect, groups of cells with similar bulk resistivities of 1.5–2.0Ωcm were chosen and measured ten times and the average values compared, as shown in Table 4. The LID test was performed for up to 40 hours, after which no further change in performance could be measured. No impacts of wafer supplier, quality or texturing on changes in I_{sc} and V_{oc} in response to LID were observed for mono-cast wafers, and no change in FF was observed for selected cells. As shown in Fig. 6, after the LID test, the efficiency levels for the best high-class mono-cast material were the same as for the CZ material.

Conclusion

For screen-printing technology, mono-cast material has significant potential for achieving an enhanced cell efficiency of more than 18%, an increase in V_{oc} of up to 9mV, and an increase in I_{sc} of more than 400mA. There are two areas of improvement: first, better bulk properties, with potential efficiency improvement of up to 0.6% absolute; and, second, an increase in efficiency of up to 0.8% absolute because of the possibility of performing anisotropic texturing for wafers with <100> crystal orientation, and further reducing reflectance.

There are new anisotropic texturing methods under development that would eliminate potential cosmetic issues with shiny areas where crystal orientation is not <100>. Improved bulk properties are a main factor for realizing gains in V_{oc} , because of the reduced number of grain and sub-grain boundaries. However, this is valid only for mono-cast material that does not have a greater number of dislocations compared to multicrystalline wafers. High I_{sc} performance comes partially from improved bulk properties, but more significantly from crystal orientation and reduced reflectance with anisotropic texturing. A V_{oc} of 632mV, an I_{sc} of above 9A, and an efficiency of 18.42% have been demonstrated. The low LID of mono-like material raises the level of performance of the best quality mono-cast cells to that of CZ mono cells.

The importance of a better classification has already been discussed [18–20] and is further emphasized in this work. However, further improvements in bulk material quality, and a higher share at the ingot level of premium-grade material with <100> crystal orientation, are essential, in order for mono-cast material suppliers to reach the

challenging targets stated in the ITRPV [1].

Acknowledgement

The author would like to thank the Photovoltech team for their outstanding support: the process engineering and production group with production runs, G. Leys from the R&D group with pilot-scale runs, Dr. A. Ristow with the PLpix system set-up and image analysis, and Dr. J. Szlufcik for helpful discussions and reviewing this paper.

References

- [1] Fischer, M. et al. 2012, "SEMI international technology roadmap for photovoltaics (ITRPV) – Challenges in c-Si technology for suppliers and manufacturers", *Proc. 27th EU PVSEC*, Frankfurt, Germany.
- [2] Shur, J. et al. 2011, "Growth of multicrystalline silicon ingot by improved directional solidification process based on numerical simulation", *Solar Energy Mater. & Solar Cells*, Vol. 95, pp. 3159–3164.
- [3] Stoddard, N. et al. 2008, "Casting single crystal silicon: Novel defect profiles from BP Solar's Mono² wafers", *Solid State Phenom.*, Vol. 131–133, pp. 1–8.
- [4] Nakajima, K. 2010, "High efficiency solar cells obtained from small size ingots with 30cm⁰ by controlling the distribution and orientation of dendrite crystals grown along the bottom of the ingot", *Proc. 25th EU PVSEC*, Valencia, Spain, pp. 1299–1301.
- [5] Nakajima, K et al. 2009, "Control of microstructures and crystal defects in Si multicrystals grown by the casting method – How to improve the quality of multicrystals to the level of single crystals", *Proc. 24th EU PVSEC*, Hamburg, Germany.
- [6] GT Advanced Technologies 2012, Press Release: "DSS" 450 MonoCast" monocrystalline growth system" [available online at <http://www.gtat.com>].
- [7] GCL-Poly 2011, Press Release: "Technology leads the future. GCL-Poly launches strongly 'GCL quasi-mono wafer'" [available online at http://www.gcl-poly.com.hk/uploadfiles/news/1351747767_fQjzbJaj06.pdf].
- [8] Beringov, S. et al. 2012, "Mono-like ingot/wafers made of solar-grade silicon for solar cells applications", *Proc. 27th EU PVSEC*, Frankfurt, Germany.
- [9] Marie, B. et al. 2011, "Seeded grown mono-like Si ingots: Effect on recombination activity of dislocations", *Proc. 26th EU PVSEC*, Hamburg, Germany.
- [10] Jouini, A. et al. 2012, "Improved multicrystalline silicon ingot crystal quality through seed growth for high efficiency solar cells", *Prog. Photovolt.: Res. Appl.*, Vol. 20, No. 6, pp. 735–746.
- [11] McMillan, W. et al. 2010, "In-line monitoring of electrical wafer quality using photoluminescence imaging", *Proc. 25th EU PVSEC*, Valencia, Spain.
- [12] Prajapati, V. et al. 2009, "High efficiency industrial silicon solar cells on silicon Mono2TM cast material using dielectric passivation and local BSF", *Proc. 24th EU PVSEC*, Hamburg, Germany.
- [13] Müller, J.W. et al. 2012, "Current status of Q.Cells' high-efficiency QANTUM technology with new world record module results", *Proc. 27th EU PVSEC*, Frankfurt, Germany.
- [14] Jay, F. et al. 2012, "20.2% efficiency with a-Si:H/C-Si heterojunction solar cells on mono like substrates", *Proc. 27th EU PVSEC*, Frankfurt, Germany.
- [15] Patzig-Klein, S. et al. 2012, "Overview of wet chemical texturing processes for 'cast-mono' silicon materials", *Proc. 27th EU PVSEC*, Frankfurt, Germany.
- [16] Ta-Ming, K. et al. 2012, "Optimisation of surface texturing to minimize surface reflectance of high efficiency mono-like silicon solar cells", *Proc. 27th EU PVSEC*, Frankfurt, Germany.
- [17] Sachs, E. et al. 2012, "1366 TextureTM: Double deep honeycomb light trapping texture", *Proc. 27th EU PVSEC*, Frankfurt, Germany.
- [18] Petter, K. et al. 2012, "Analysis of mono-cast silicon wafer and solar cells", *Proc. 27th EU PVSEC*, Frankfurt, Germany.
- [19] Caley, N. 2011, "Cast-mono wafers revisited: Re-emergence of mono tech driving wafering innovations", *Solar Industry* (September), pp. 36–40.
- [20] Kaden, T. et al. 2012, "Analysis of mono-cast silicon wafers and solar cells on industrial scale", *Proc. 2nd SiliconPV Conf.*, Leuven, Belgium.

About the Author

Milica Mrcarica received her MEngSc in photovoltaics from the University of New South Wales (UNSW), Australia. From 1995 to 2009 she was with BP Solar not only working on but also leading a wide range of engineering and R&D projects and technology scale-up. After that Milica was a process manager for screen-printing and LDSE technology with Roth&Rau R&D group. In 2011 she joined the Photovoltech R&D team, where she has been in charge of Si wafer evaluation and emitter development for standard and high-efficiency cell concepts.

Enquiries

Photovoltech NV
18 Grijspenlaan
3300 Tienen
Belgium

Tel: +32 (0) 472185443
Email: milica.mrcarica@yahoo.com